ISSN 1749-3889 (print), 1749-3897 (online)
International Journal of Nonlinear Science
Vol.12(2011) No.1,pp.86-94

Stability Analysis of Dual Solutions in Stagnation-point Flow and Heat Transfer over a Power-law Shrinking Surface

T. Ray Mahapatra[1] *, S.K. Nandy[2]
[1]Department of Mathematics, Visva-Bharati, Santiniketan-731 235, India.
[2]Department of Mathematics, A.K.P.C Mahavidyalaya, Bengai, Hooghly -712 611, India.
(Received 3 March 2011, accepted 4 June 2011)

Abstract: An analysis is made of two-dimensional stagnation-point flow and heat transfer in a viscous fluid over a nonlinearly shrinking sheet. The governing partial differential equations are transformed into ordinary differential equations using similarity transformation, before being solved numerically by the shooting method. This investigation explores the conditions of existence and uniqueness of the similarity solution. It is found that dual solutions exist for a certain range of α, the ratio of shrinking velocity and free stream velocity. A linear stability analysis reveals that one solution is linearly stable while the other is linearly unstable. The features of the flow and heat transfer characteristics for different physical parameters are analyzed and discussed. Quite different flow behaviour is observed for a nonlinearly shrinking sheet from a nonlinearly stretching sheet.

Keywords: stagnation-point flow; nonlinearly shrinking sheet; dual solutions; stability analysis; heat transfer

1 Introduction

Stagnation flow of an incompressible viscous fluid over a stretching or shrinking sheet has important practical applications in engineering and manufacturing processes, namely continuous casting, glass fibre production, metal extrusion, hot rolling of paper, textiles and wire drawing. Hiemenz [1] was first to study the two-dimensional stagnation-point flow towards a stationary plate. The axisymmetric three dimensional stagnation flow was discussed by Homann [2]. Thereafter various aspects of stagnation flow and heat transfer were considered by many researchers (Chiam [3], Mahapatra and Gupta [4, 5], Ishak et al. [6] and Wang [7]). Most of these investigations are on the flow due to linear stretching sheet. However Gupta and Gupta [8] have underlined that the stretching of the sheet may not necessarily be linear. In view of this, Vajravelu [9] studied flow and heat transfer in a viscous fluid over a nonlinearly stretching sheet without viscous dissipation. Cortell [10] discussed the numerical solution for viscous flow and heat transfer over a nonlinearly stretching sheet by considering the viscous dissipation. Recently Abbas and Hayat [11] investigated stagnation slip flow and heat transfer characteristics of a viscous fluid over a nonlinearly stretching sheet.

Recently, the boundary layer flow due to a shrinking sheet has attracted considerable interest. For this flow configuration, the fluid is attracted towards a slot and the flow is quite different from the stretching case. From a physical point of view, vorticity generated at the shrinking sheet is not confined within a boundary layer and a steady flow is not possible unless adequate suction is applied at the sheet. For this new type of shrinking flow, it is essentially a backward flow as discussed by Goldstein [12]. For a backward flow configuration, the fluid losses memory of the perturbation introduced by the slot. As a result, the flow induced by the shrinking sheet shows quite distinct physical phenomena from the forward stretching case.

Miklavcic and Wang [13] investigated both two-dimensional and axisymmetric viscous flow induced by a shrinking sheet in the presence of uniform suction. This problem was then extended to magnetohydrodynamic (MHD) flow by Sajid and Hayat [14]. Fang and Zhang [15] successfully obtained the closed form analytic solution for steady MHD flow over a shrinking sheet subjected to applied suction and they reported greatly different solution behaviour with multiple solution branches compared to the corresponding stretching sheet problem. The boundary layer flow over a continuously shrinking

* **Corresponding author**. *E-mail address*: trmahapatra@yahoo.com

IJNS.2011.08.15/516

sheet with a power law surface velocity and mass transfer were investigated by Fang [16]. The unsteady viscous flow over a continuously shrinking surface with mass suction was also investigated by Fang et al. [17].

Steady two-dimensional and axisymmetric stagnation point flow with heat transfer over a shrinking sheet was investigated by Wang [18]. The above shrinking sheet problem for the micropolar fluid was studied by Ishak et al. [19]. Very recently, Mahapatra et al. [20] investigated the MHD stagnation point flow and heat transfer over a shrinking sheet, the flow being permeated by a uniform transverse magnetic field. Note that with an added stagnation flow to contain the vorticity, similarity solution is possible even in the absence of suction at the surface.

In this article, the steady two-dimensional stagnation point flow and heat transfer of a viscous incompressible fluid over a nonlinearly shrinking sheet is investigated. Results for velocity, temperature, skin friction coefficient and rate of heat transfer are examined. A linear stability analysis of the dual solutions is discussed. To the best of our knowledge, this problem is not studied before and therefore the results obtained are new.

2 Flow analysis

Consider the steady two-dimensional laminar stagnation-point flow of a viscous incompressible fluid towards a nonlinear shrinking sheet. The x-axis runs along the shrinking surface in the direction opposite to the sheet motion and y-axis is perpendicular to it. It is assumed that the potential stagnation flow at infinity is given by $U = ax^n$, $V = -anx^{n-1}y$ where $a(> 0)$ is the strength of the stagnation flow and n is an exponent. On the sheet, the velocity components are $u = cx^n$, $v = 0$, where $c(< 0)$ is the shrinking rate (stretching rate if $c > 0$).

Based on the boundary layer assumption, the governing equations of this problem become

$$\frac{\partial u}{\partial x} + \frac{\partial v}{\partial y} = 0\,, \tag{1}$$

$$u\frac{\partial u}{\partial x} + v\frac{\partial u}{\partial y} = U(x)\frac{dU}{dx} + \nu\frac{\partial^2 u}{\partial y^2}\,, \tag{2}$$

where (u, v) are the velocity components in the x and y directions, respectively and ν is the kinematic viscosity. The boundary conditions for the above flow situation are

$$u = u_w = cx^n\,, \qquad v = v_w = 0 \qquad \text{at} \quad \text{y} = 0\,, \tag{3}$$

and

$$u \to U(x) = ax^n \qquad \text{as y} \to \infty\,. \tag{4}$$

Defining relevant dimensionless quantities

$$u(x,y) = ax^n F'(\eta)\,, \quad v(x,y) = -x^{(n-1)/2}\sqrt{\frac{a\nu(n+1)}{2}}\left[F(\eta) + \left(\frac{n-1}{n+1}\right)\eta F'(\eta)\right]\,,$$
$$\eta = y\sqrt{\frac{a(n+1)}{2\nu}}x^{(n-1)/2}\,, \tag{5}$$

and substituting into Eqs. (1) and (2) we get

$$F''' + FF'' - \left(\frac{2n}{n+1}\right)F'^2 + \left(\frac{2n}{n+1}\right) = 0, \tag{6}$$

where a prime denotes differentiation with respect to the similarity variable η. The boundary conditions (3) and (4) becomes

$$F = 0, \quad F' = c/a = \alpha(say) \qquad \text{at} \quad \eta = 0, \tag{7}$$

$$F' \to 1 \quad \text{as} \quad \eta \to \infty\,. \tag{8}$$

Eqs. (6)- (8) for $n = 1$ (i.e., for linear shrinking boundary problem) has been carried out by Wang [18].

The dimensionless velocity components can be written from Eq. (5) as

$$u^* = \frac{u}{\left(a^{1/n}\frac{2\nu}{n+1}\right)^{n/(n+1)}} = \xi^{2n/(n+1)}F'(\eta)\,, \tag{9}$$

and

$$v^* = \frac{v}{\left(a^{1/n}\frac{2\nu}{n+1}\right)^{n/(n+1)}} = -\xi^{(n-1)/(n+1)}V(\eta) \tag{10}$$

where

$$\xi = \left(\frac{a(n+1)}{2\nu}\right)^{1/2} x^{(n+1)/2}\ ,\ V(\eta) = \frac{1}{2}[(n+1)F(\eta) + (n-1)\eta F'(\eta)]\ . \tag{11}$$

The shear stress at the stretched surface is defined as

$$\begin{aligned}\tau_w &= \mu\left[\frac{\partial u}{\partial y}\right]_{y=0}\\ &= a\mu\sqrt{\frac{a(n+1)}{2\nu}}x^{(3n-1)/2}F''(0)\ .\end{aligned} \tag{12}$$

where μ (assumed constant) is the viscosity of the fluid.

3 Heat transfer

Using the boundary layer approximations and taking into account the viscous dissipation, the equation of the energy for temperature T is given by

$$u\frac{\partial T}{\partial x} + v\frac{\partial T}{\partial y} = \kappa\frac{\partial^2 T}{\partial y^2} + \frac{\mu}{\rho c_p}\left(\frac{\partial u}{\partial y}\right)^2\ , \tag{13}$$

where κ and c_p and ρ denote the thermal diffusivity, specific heat at constant pressure and density of the fluid respectively. The last term in Eq. (13) represents the viscous dissipation in the boundary layer approximation. The boundary conditions are

$$T = T_w \quad \text{at} \quad \mathrm{y = 0} \quad \text{and} \quad \mathrm{T = T_\infty} \quad \text{as} \quad \mathrm{y \to \infty}\ , \tag{14}$$

where T_w and T_∞ are constants and we assume that $T_w > T_\infty$. Define the dimensionless temperature $\theta(\eta)$ as

$$\theta(\eta) = \frac{T - T_\infty}{T_w - T_\infty}\ . \tag{15}$$

Substituting Eqs. (5) and (15) into Eq. (13), we get

$$\theta'' + PrF\theta' + PrE_c\alpha^2 F''^2 = 0\ , \tag{16}$$

where $E_c(= u_w^2/c_p(T_w - T_\infty))$ is the Eckert number, $Pr(= \nu/\kappa)$ is the Prandtl number. It should be noted that the temperature profile always depend on x i.e., one may look for the availability of local similarity solution. The boundary conditions for $\theta(\eta)$ are obtained from Eq. (14) as

$$\theta(0) = 1 \qquad \text{and} \qquad \theta(\infty) = 0\ . \tag{17}$$

The rate of heat transfer of the surface is defined from Eq. (15) as

$$-\lambda_T\left(\frac{dT}{dy}\right)_{y=0} = -\lambda_T(T_w - T_\infty)\theta'(0)x^{(n-1)/2}\sqrt{\frac{a(n+1)}{2\nu}}\ , \tag{18}$$

where λ_T is the thermal conductivity.

4 Numerical Solution

An analytical solution for the flow problem with $n \neq 0$ does not exist and hence one has to use numerical technique. So Eqs. (6)-(8) are solved numerically by an efficient Shooting method for different values of the parameters. To do this, we first transform the non-linear differential equation (6) to a system of three first order differential equations as :

$$\begin{aligned} &y_1' = y_2\ , y_2' = y_3\ ,\\ &y_3' = \frac{2n}{n+1}y_2^2 - y_1y_3 - \frac{2n}{n+1}\ ,\end{aligned} \tag{19}$$

where $y_1 = F(\eta)$, $y_2 = F'(\eta)$, $y_3 = F''(\eta)$ and a prime denotes differentiation with respect to the independent variable η. The boundary conditions (7) and (8) become

$$y_1 = 0\,, \quad y_2 = \alpha \quad \text{at} \quad \eta = 0\,, \qquad y_2 \to 1 \quad \text{as} \quad \eta \to \infty\,. \tag{20}$$

For a given α, the values of y_1 and y_2 are known at the starting point $\eta = 0$. Now the value of y_2 as $\eta \to \infty$ is replaced by $y_2 = 1$ at a finite value $\eta = \eta_\infty$ to be determined later. The value of y_3 at $\eta = 0$ is guessed in order to initiate the integration scheme. Starting from the given values of y_1 and y_2 at $\eta = 0$ and the guessed value of y_3 at $\eta = 0$, we integrate the first order equations (19) by using a fourth-order Runge-Kutta method up to the end-point $\eta = \eta_\infty$. The computed value of y_2 at $\eta = \eta_\infty$ is then compared with $y_2 = 1$ at $\eta = \eta_\infty$. The absolute difference between these two values should be as small as possible. To this end we use a Newton-Raphson iteration procedure to assure quadratic convergence of the iterations. The value of η_∞ is then increased till y_2 attains the value 1 asymptotically. The value $\eta_\infty = 12$ was found to be adequate for all the ranges of parameters studied here.

Using the numerical values of $F(\eta)$ from the solution of Eqs. (6)- (8) , Eqs. (16) along with the boundary conditions (17) are solved numerically using the same method as described above to obtain $\theta(\eta)$.

5 Stability analysis

Our numerically results show that for a certain range of α, there exist two branches of solutions for different values of n. So we have to test the stability of the dual solutions. To do this, we consider the unsteady form of Eq. (6) as

$$\frac{\partial u}{\partial t} + u\frac{\partial u}{\partial x} + v\frac{\partial u}{\partial y} = U(x)\frac{dU}{dx} + \nu\frac{\partial^2 u}{\partial y^2}\,. \tag{21}$$

The unsteady similarity solution can be taken in the form

$$u(x,y) = ax^n f_\eta(\eta,\tau)\,, \qquad v = -x^{(n-1)/2}\sqrt{\frac{a\nu(n+1)}{2}}\left[f + \left(\frac{n-1}{n+1}\right)\eta f_\eta - \frac{2}{n+1}\alpha\tau f_\tau\right]\,, \tag{22}$$

where η is same as defined in Eq. (5) and $\tau = atx^{-\alpha}$ is the time. Here a subscript denotes differentiation with respect to the subscripted variable. Substituting (22) into (21), we see that similarity is obtained when $\alpha = 1 - n$ and in that case $\tau = atx^{n-1}$. Hence the governing equation (21) becomes

$$f_{\eta\eta\eta} + ff_{\eta\eta} - \left(\frac{2n}{n+1}\right)f_\eta^2 + 2\left(\frac{1-n}{1+n}\right)\tau\left[f_\eta f_{\tau\eta} - f_\tau f_{\eta\eta}\right] - \left(\frac{2}{n+1}\right)f_{\tau\eta} + \frac{2n}{n+1} = 0\,, \tag{23}$$

The boundary conditions become

$$f(0,\tau) = 0, \qquad f_\eta(0,\tau) = 1, \qquad f_\eta(\infty,\tau) = 0 \tag{24}$$

Stability of the dual solutions are determined by adopting the stability analysis of Merkin [21] and we put

$$f(\eta,\tau) = F(\eta) + e^{-\gamma\tau}g(\eta,\tau)\,, \tag{25}$$

where $F(\eta)$ satisfies the steady state boundary value problem (6) and γ is the small disturbances of growth (or decay) rate. Here $g(\eta,\tau)$ and all its derivatives are assumed small compared with the steady solution $F(\eta)$ and its derivatives. Such an assumption is made because we are studying the linear stability analysis of the basic flow $F(\eta)$. Inserting the time-dependent solution (25) into (23) and (24), linearization furnishes the eigen-value problem

$$g_{\eta\eta\eta} + Fg_{\eta\eta} + F_{\eta\eta}g - \left(\frac{4n}{n+1}\right)F_\eta g_\eta + 2\left(\frac{1-n}{1+n}\right)\tau\left[F_\eta(g_{\tau\eta} - \gamma g_\eta) - F_{\eta\eta}(g_\tau - \gamma g)\right] - \frac{2}{1+n}(g_{\tau\eta} - \gamma g_\eta) = 0\,, \tag{26}$$

and

$$g(0,\tau) = 0, \qquad g_\eta(0,\tau) = 0, \qquad g_\eta(\infty,\tau) = 0. \tag{27}$$

To identify initial growth or decay of the solution (25), we take $\tau = 0$, and hence $g = g_0(\eta)$. So to test our numerical procedure, we solved the linear eigenvalue problem

$$g_0''' + Fg_0'' + \frac{1}{n+1}(2\gamma - 4nF')g_0' + F''g_0 = 0\ , \tag{28}$$

and

$$g_0(0) = 0, \quad g_0'(0) = 0, \quad g_0'(\infty) = 0, \tag{29}$$

where a prime denotes differentiation with respect to the similarity variable η. The function $F(\eta)$ is obtained from the steady state boundary layer Eqs. (6)-(8). Using the numerical values of $F(\eta)$, Eqs. (28)-(29) are solved numerically. Solutions of (28) and (29) give an infinite set of eigen-values $\gamma_1 < \gamma_2 < \gamma_3 < \cdots$, if the smallest eigen-value γ_1 is positive, then there is an initial decay of disturbances and the flow is stable. On the other hand when γ_1 is negative, there is an initial growth of disturbances and the flow is unstable. A detailed explanation of the stability analysis method is given in [22].

6 Results and discussion

To validate our solution, we make a comparison of the values of $F''(0)$ for different values of α with $n = 1$ with the results obtained by Wang [18] who studied the stagnation point flow towards a linearly shrinking sheet and is shown in Table 1. Good agreement is observed between these two results.

Our numerical results reveal that the existence and uniqueness of the solution depend on n in addition with α. Fig. 1 shows the trajectories of the values of $F''(0)$ for different values of n. In this figure, the solutions represented by the solid lines are designated as first solution branch and those by the dashed line are designated as second solution branch. Numerically it is seen that for $n = 0.5$, the solution is unique for $\alpha > -1$, dual solutions for $-1.099262 \le \alpha \le -1.0$ and no similarity solution is found for $\alpha < -1.099262$. Again for $n = 1.0$, the solution is unique for $\alpha > -1$, for $-1.2465 \le \alpha \le -1.0$ there exists dual solutions and for $\alpha < -1.2465$ no similarity solution exists. The results for $n = 1.0$ agree well with those of Wang [18]. However for $n = 1.5$, the solution is unique for $\alpha > -1$, dual solutions for $-1.312372 \le \alpha \le -1.0$ and no similarity solution is found for $\alpha < -1.312372$. Thus we find that, the range of unique solution remains same (i.e., $\alpha > -1$) for all n but the existence range of similarity solution significantly increases with increase in n and consequently dual solutions range increases with increase in n.

The horizontal and vertical velocity profiles for several values of the parameters are shown in Figs 2-5. In Fig. 2 the dual horizontal velocity profiles (i.e.,$F'(\eta)$) show that the velocity increases with increase in n for the first solution and it decreases with increase in n for the second solution. Fig. 3 shows that $|F'(\eta)|$ decreases as $|\alpha|$ increases for first solution and for the second solution, it increases as $|\alpha|$ increases. Figs. 4 and 5 display the variation of the vertical velocity component $V(\eta)$ for different values of n and α respectively. It is interesting to note that $V(\eta)$ in initially decreasing with values being negative and for large η, it starts to increase and ultimately it becomes positive. Hence for all $\alpha(< 0)$, the velocity profiles exhibit reverse flow. This is caused due to the opposite directions of shrinking and free stream velocities. Fig. 4 shows that in the first solution reverse flow region decreases as n increases and on the other hand , for the second solution this region increases as n increases in certain initial range of η and decreases after that. Fig. 5 demonstrates that the region of reverse flow increases as $|\alpha|$ increases for the first solution and decreases for the second solution.

Fig. 6 shows the variation of the smallest eigenvalue γ_1 with α for several values of n. In this figure the smallest eigenvalue γ_1 for the first solution is plotted by solid line and that for the second solution is plotted by dotted line. Since for the first solution, γ_1 is real and positive, it follows that the first solution is linearly stable. Also for a given value of α, γ_1 increases with increase in n. Thus we may say that for these stable solutions, disturbances decay more quickly with increase in n. Since for the second solution , γ_1 is real and negative, it is clear that the second solution is linearly unstable. For this solution γ_1 decreases with increase in n (for a fixed α) and hence the solution is more unstable with increasing n.

To see the variations of the parameter n, α, the Eckert number E_c and the Prandtl number Pr on the temperature profile θ, Figs. 7-10 are plotted. Fig. 7 shows the effect of n on the temperature θ. The thermal boundary layer decreases as n increases for the first solution but opposite effects are observed for the second solution. Fig. 8 illustrates the effect of α on the temperature θ. In this case the thermal boundary layer increases as $|\alpha|$ increases for the first solution and completely opposite behaviour is observed for the second solution. Fig. 9 shows the influence of E_c on the temperature field θ. The figure shows that the temperature at a point increases with increase in E_c. From a physical point of view, this follows from the fact that an increase in E_c implies increase in viscous dissipation leading to rise in temperature of the fluid. The consequence of Pr on temperature distribution is shown in Fig. 10. It is observed that near the sheet, temperature at a point increases with increase in Pr but beyond this increase in Pr causes decrease in temperature as well as thermal boundary layer thickness. The variation of the dimensionless surface heat flux $-\theta'(0)$ against α for different values of n is displayed in Fig. 11. In this figure, dual nature of the temperature is observed. The figure reveals that the magnitude of surface heat flux decreases as n increases for the first solution whereas it increases with increase in n for the second solution.

Table 1: Values of $F''(0)$ for the shrinking sheet when $n = 1$

	Wang [18]		Present work	
α	first solution	second solution	first solution	second solution
-0.25	1.40224	-	1.402242	-
-0.50	1.49567	-	1.495672	-
-0.75	1.48930	-	1.489296	-
-1.00	1.32882	0.0	1.328819	0.0
-1.10	-	-	1.186680	0.049229
-1.15	1.08223	0.116702	1.082232	0.116702
-1.20	-	-	0.932470	0.233648
-1.2465	0.55430	-	0.584374	0.554215

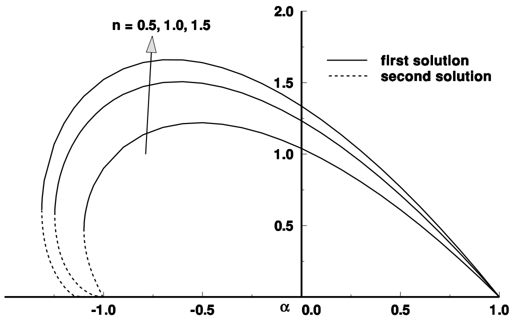

Figure 1: Wall shear stress $F''(0)$ versus α for different n.

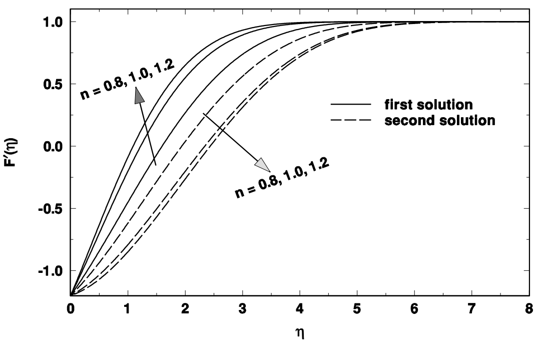

Figure 2: Variation of $F'(\eta)$ with η for several values of n with $\alpha = -1.2$.

7 Conclusion

We have theoretically studied the similarity solutions for steady two-dimensional stagnation-point flow over a non-linearly shrinking sheet. The transformed nonlinear ordinary differential equations have been solved numerically using shooting method. Different from a nonlinearly stretching sheet, it is found that the solutions for a nonlinearly shrinking sheet are non-unique. Enhancement of n causes the more increment in the existence range of similarity solution and the range of dual solutions. Moreover the boundary layer thickness of the velocity as well as thermal in the first solution are always smaller than of the second solution.

Acknowledgement

The work of one of the authors (T.R.M) is supported under SAP (DRS PHASE II) program of UGC, New Delhi, India.

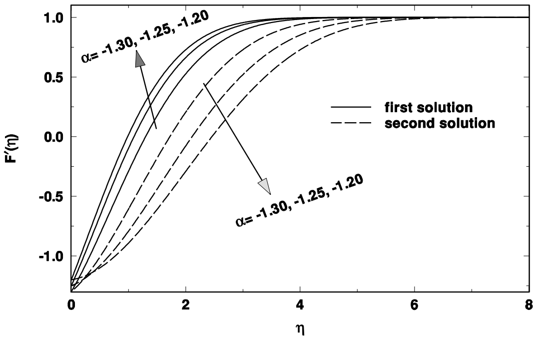

Figure 3: Variation of $F'(\eta)$ with η for several values of $\alpha(< 0)$ with $n = 1.5$.

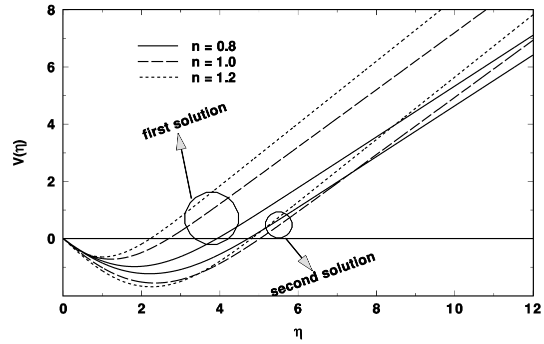

Figure 4: Variation of $V(\eta)$ with η for several values of n with $\alpha = -1.2$.

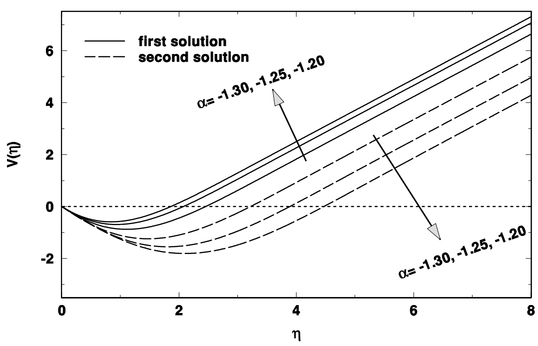

Figure 5: Variation of $V(\eta)$ with η for several values of $\alpha(< 0)$ with $n = 1.5$.

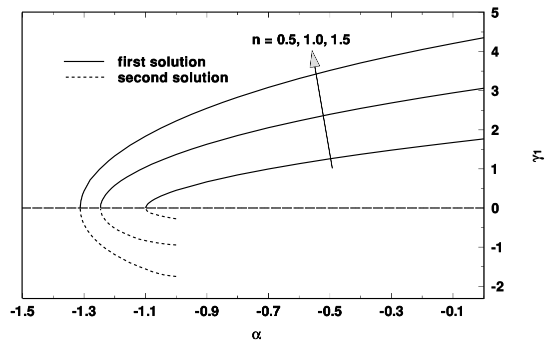

Figure 6: Plot of lowest eigenvalues γ_1 as a function of α for different values of n.

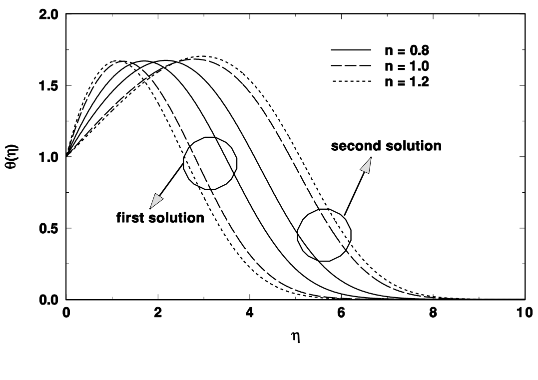

Figure 7: Variation of $\theta(\eta)$ with η for several values of n with $\alpha = -1.2$, $Pr = 0.7$ and $E_c = 1.5$.

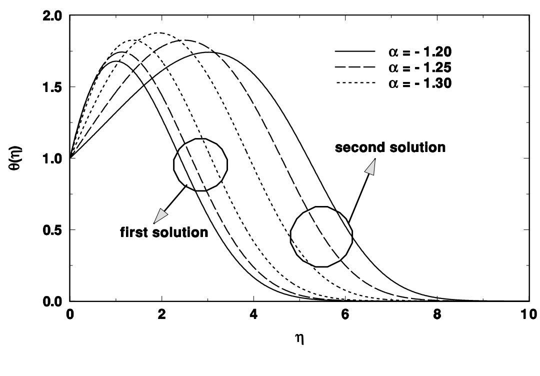

Figure 8: Variation of $\theta(\eta)$ with η for several values of $\alpha(< 0)$ with $n = 1.5$, $Pr = 0.7$ and $E_c = 1.5$.

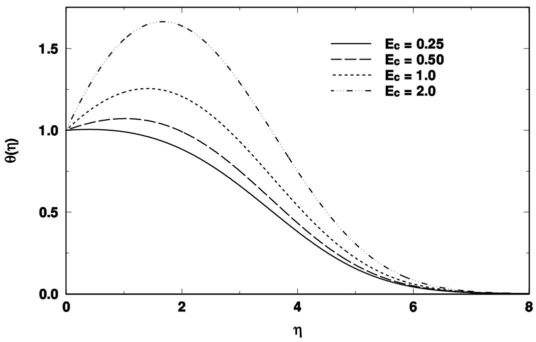

Figure 9: Variation of $\theta(\eta)$ with η for several values of Eckert number E_c with $n = 0.8$, $Pr = 0.5$ and $\alpha = -1.2$.

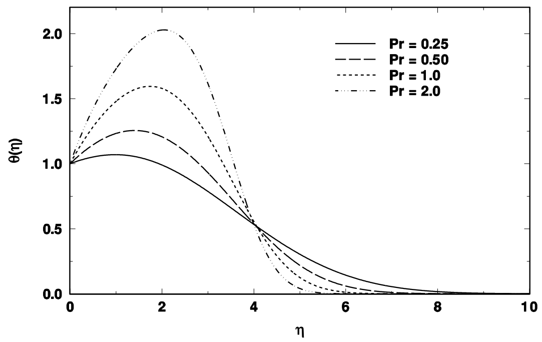

Figure 10: Variation of $\theta(\eta)$ with η for several values of Prandtl number Pr with $n = 0.8$, $E_c = 1.0$ and $\alpha = -1.2$.

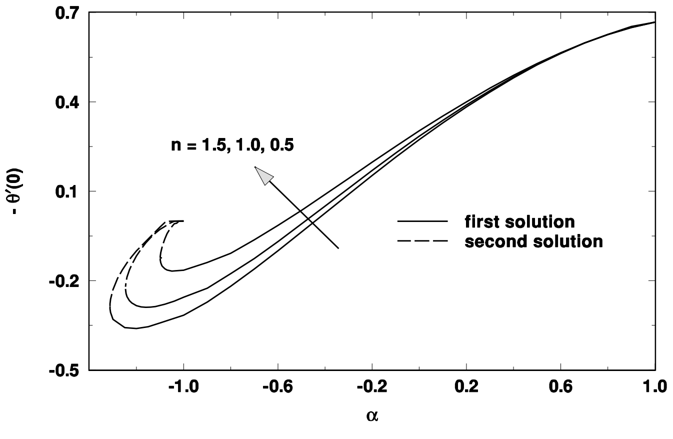

Figure 11: Variation of $-\theta'(0)$ with α for several values of n with $Pr = 0.7$ and $E_c = 0.5$.

References

[1] K. Hiemenz. Die Grenzschicht in Einem in Dem Gleichformingen Flussigkeitsstrom Eingetauchten Gerade Kreiszlinder. *Dingler Polytech J.*, 326(1911): 321-410.

[2] F. Homann. Der Einfluss Grosser Zahighkeit Bei Der Stromung um den Zylinder und um die Kugel. *Zeit. angew. Math. Mech.*, 16(1936): 153-164.

[3] T.C. Chiam. Stagnation-point flow towards a stretching plate. *J. Phys. Soc. Japan*, 63(1994): 2443-2444.

[4] T.R. Mahapatra and A.S. Gupta. Heat transfer in stagnation- point flow towards a stretching sheet. *Heat Mass Transfer*, 38(2002): 517-521.

[5] T.R. Mahapatra and A.S. Gupta. Stagnation-point flow towards a stretching surface. *Can. J. Chem. Eng.*, 81(2003): 258-263.

[6] A. Ishak, R. Nazar, I. Pop. Mixed convection boundary layer in the stagnation point flow towards a stretching vertical sheet. *Meccanica*, 41(2006): 509-518.

[7] C.Y. Wang. Liquid film on an unsteady stretching sheet. *Quarterly of Appl. Math.*, 48(1990)(4): 601-610.

[8] P.S. Gupta and A.S. Gupta. Heat and mass transfer on a stretching sheet with suction or blowing. *Can. J. Chem. Eng.*, 55(1977): 744-746.

[9] K. Vajravelu. Viscous flow over a non-linearly stretching sheet. *Appl. Math. Comput.*, 124(2001): 281-288.

[10] R. Cortell. Viscous flow and heat transfer over a non-linearly stretching sheet. *Appl. Math. Comput.*, 184(2007): 864-873.

[11] Z. Abbas and T. Hayat. Stagnation slip flow and heat transfer over a nonlinear stretching sheet. *Numerical methods for Partial Differential Equations*, doi:10.1002/num.20523, (2009).

[12] S. Goldstein. On backward boundary layers and flow in converging passages. *J. Fluid Mech.*, 21(1965): 33-45.

[13] M. Miklavcic and C.Y. Wang. Viscous flow due to a shrinking sheet. *Quart. Appl. Math.*, 64(2006)(2): 283-290.

[14] M. Sajid and T. Hayat. The application of homotopy analysis method for MHD viscous flow due to a shrinking sheet. *Chaos Solitons Fractals*, 39(2009): 1317-1323.

[15] T. Fang and J. Zhang. Closed form exact solution of MHD viscous flow over a shrinking sheet. *Commun. Nonlinear Sci. Numer. Simulation*, 14(2009): 2853-2857.

[16] T. Fang. Boundary layer flow over a shrinking sheet with power-law velocity. *Int. J. Heat Mass Transfer*, 51(2008)(25-26): 5838-5843.

[17] T. Fang, J. Zhang and S. Yao. Viscous flow over an unsteady shrinking sheet with mass transfer. *Chinese Phys. Lett.*, 26(2009)(1): 014703.

[18] C.Y. Wang. Stagnation flow towards a shrinking sheet. *Int. J. Nonlinear Mech.*, 43(2008): 377-382.

[19] A. Ishak, Y.Y. Lok, I. Pop. Stagnation-point flow over a shrinking sheet in a micropolar fluid. *Chem. Eng. Comm.*, 197(2010):1417-1427.

[20] T.R. Mahapatra, S.K. Nandy and A.S. Gupta. Momentum and heat transfer in MHD stagnation-point flow over a shrinking sheet. *J. Appl. Mech. Trans. ASME* 78(2011), 021015.

[21] J.H. Merkin. Mixed convection boundary layer flow on a vertical surface in a saturated porous medium. *J. Eng. Math.*, 14(1980): 301-313.

[22] T.R. Mahapatra, S.K. Nandy and A.S. Gupta. Dual solution of MHD stagnation-point flow towards a stretching surface. *Engineering*, 2(2010): 299-305.